ELSEVIER

European Polymer Journal 37 (2001) 349–360

EUROPEAN POLYMER JOURNAL

Tertiary phosphine complexes of nickel(II) thiocyanate: an evaluation of the photostabilisation of polystyrene

M. Edge, P. Faulds, D.G. Kelly *, A. McMahon, G.C. Ranger, D. Turner

Department of Chemistry and Materials, Manchester Metropolitan University, Chester Street, Manchester M1 5GD, UK

Received 21 July 1999; received in revised form 21 December 1999; accepted 12 May 2000

Abstract

Polystyrene films have been prepared incorporating zinc stearate and nickel(II) thiocyanate complexes of methyldiphenyl- and alkenyldiphenyl-phosphines (alkenyl = vinyl, allyl, but-3-enyl, pent-4-enyl). Investigation of the thermal and fluorescence properties of the nickel complexes indicates high thermal stability and minimal photochemical activity. Polymer films containing the zinc and nickel complexes were photodegraded under artificial conditions and referenced to a similarly exposed nickel-free standard. The degradation of films containing nickel additives and the nickel-free standard was assessed using diffuse reflectance IR spectroscopy, CIELab colour space and $^{31}P\{^{1}H\}$ NMR. Within the polymer films nickel complexes do not degrade at a significantly greater rate than the polymer matrix, and whilst those containing vinyl, but-3-enyl and pent-4-enyl functions appear passive (displaying neither photosensitisation nor photostabilisation), methyl and allyl substituted complexes do offer significant stabilisation. Phosphine oxide species are identified by $^{31}P\{^{1}H\}$ NMR as the principal decomposition products, suggesting that peroxide oxidation of co-ordinated phosphines may represent the principal mode of photostabilisation. Assessments of colour space fastness on exposure to aqueous, acidic and alkaline media were made. These indicate comparable decomposition of nickel(II) thiocyanate and zinc stearate complexes in all three environments, suggesting that hydrolytic processes predominate in complex decomposition.

Keywords: Polystyrene; Photostabilisation; Nickel; Phosphine

1. Introduction

The photostabilisation of polymers may be achieved by three principal routes; the absorbance of incident radiation, the inhibition or trapping of radicals formed by UV generated homolytic bond cleavage, or the non-radical decomposition of peroxides derived from polymerisation processes and free radical termination steps. Sterically hindered amines and phenols are the most widely employed photostabilisers in a host of products as diverse as polymers, lubricants and foodstuffs [1]. Transition metal salts and complexes may perform as multifunctional additives in polymer matrices including pigments, photostabilisers and flame retardants. Numerous complexes have been evaluated in one or more of these roles [2–4]. The choice of metal is critical; metal ion systems with relatively small redox couples such as Cu^{+}/Cu^{2+} and Fe^{2+}/Fe^{3+} are commonly associated with photosensitisation [5]. However, nickel(II) shows little propensity for one electron oxidation or reduction in most environments. It has therefore been employed in a variety of stabilisers such as (2,2′-thio-*bis*(4-*t*-octyl-phenolato) *n*-butylamine)nickel(II) (Cyasorb UV 1084, Cyanamid), *bis*(3,5-di-*t*-butyl-4-hydroxybenzylmonoethylphosphonate)nickel(II) (Irgastab 2002, Ciba) and *bis*(1-phenyl-3-methyl-4-decanoyl-5-pyrazolate)nickel(II) (Sanduvor NPU, Sandoz). Recent evaluation of fumarate and dimethylglyoximate complexes of nickel(II) suggest superior light stabilisation may be achieved

* Corresponding author. Tel.: +44-161-247-1425; fax: +44-161-247-6357.

E-mail address: d.g.kelly@mmu.ac.uk (D.G. Kelly).

0014-3057/01/$ - see front matter
PII: S0014-3057(00)00108-7

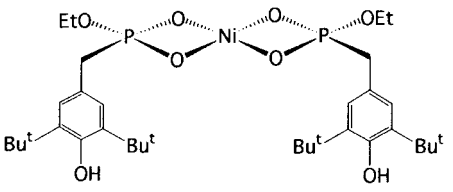

Irgastab 2002

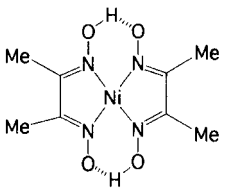

Ni(dmg)$_2$ [ref. 3]

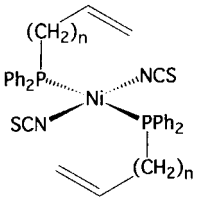

n = 0 (1), 1 (2), 2 (3), 3 (4)

Nickel(II) Phosphines [This work]

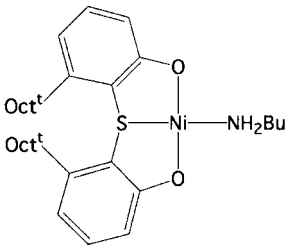

Cyasorb UV 1084

Scheme 1. Commercial and experimental nickel photostabilisers.

using these chelated complexes [3]. It is apparent that few structural similarities exist between any of these additives other than their nickel content, (Scheme 1). The origins of such limited structure/reactivity correlation may be related to the complexes' mode of action. The beneficial light stabilising properties of transition metal polymer additives has traditionally been ascribed to 'quenching' [6], i.e. the absorbance of UV radiation and dissipation through vibrational or other non-radical modes. However, detailed studies indicate the primary role of such complexes is in the decomposition of peroxides [7]. In the current study a series of nickel(II) thiocyanate complexes containing tertiary phosphine ligands, $[Ni(NCS)_2(PPh_2R)_2]$ (R = methyl, vinyl, allyl, but-3-enyl, pent-4-enyl) have been prepared and incorporated with zinc stearate into atactic polystyrene films. Such complexes combine a series of properties that make them valuable candidates for assessment as light stabilisers. They exhibit a broad range of UV absorbance bands derived from nickel-centred electronic transitions, phenyl and alkene moieties. Moreover, they belong to a class of complexes that readily react with peroxides [8–10], and as a consequence of their phosphorus content may offer additional flame retardant properties [4]. In common with many transition metal compounds, these nickel complexes display moderately intense absorbances in the visible spectrum associated with $d \rightarrow d$ transitions. Such properties hinder their application in transparent and non-pigmented systems, but such drawbacks have not inhibited the commercial use of nickel complexes in coloured packages.

2. Experimental

2.1. Reagents and complexes

Polystyrene ($d = 1.04\ g\,cm^{-3}$, melt index = 8.5) and zinc stearate (99%) were obtained from Aldrich. Solvents were Analar® grade and used without further purification. Nickel complexes were prepared by published procedures and characterised by elemental analysis, ^1H and $^{31}P\{^1H\}$ NMR, infrared spectroscopy and UV–VIS spectroscopy [15]. Reference phosphine oxides were prepared by the Oxone® oxidation of the corresponding commercially available phosphine ligands obtained from Aldrich. $[OPPh_2(CHCH_2)]_n$ was obtained by $Et_2O \cdot BF_3$ catalysed polymerisation of PPh_2- ($CH{=}CH_2$) [27,28] in toluene followed by Oxone® oxidation.

2.2. Complex characterisation

Thermogravimetric analyses were carried out for **1**–**5** using a Mettler TG50 thermobalance. Nitrogen atmospheres were employed in each case over a 50–500°C temperature programme with a heating rate of 10°C min^{-1}. Fluorescence studies were performed using a Perkin–Elmer LS50B luminescence spectrometer on 10^{-3} M solutions of **1**–**5** prepared in dry dichloromethane. Survey scans assessing total fluorescence were carried out at 10 nm increments using excitation wavelengths from 300–800 nm. In addition excitation at specific wavelengths corresponding to the unsaturated

hydrocarbon absorptions and d → d transitions were considered; both transitions appear relatively insensitive to structural modifications in **1–5** lying at ~390 and ~630 nm, respectively.

2.3. Polymer preparation

Polystyrene (10.00 g) was slurried in dry toluene (40 cm^3) for ~2 h until a homogeneous viscous fluid was formed. Zinc stearate (0.20 g) was added and quickly (~0.5 h) dispersed within the fluid. The appropriate nickel complex **1–5** (0.30 g) was added as a toluene solution (20 cm^3). The resultant homogeneous red slurry was stirred for a further 2 h after which solvent was removed in vacuo and the solid formed heated in vacuo for 4 h at 140°C. Residual toluene was analysed by thermogravimetric analysis (50–190°C, 5°C min^{-1}). If toluene content was >0.75%, the heating in vacuo was repeated. Typically two to three cycles were required. Polymers were cast to thin films, **F1–F5** respectively, using a hot melt press (140°C, 5 bar, 5 min). A reference film without metal complex was similarly prepared and designated **F0**.

2.4. Stability studies

Polymer films **F0–F5** were exposed to UV radiation using a Xenotest-150 ($\lambda \geqslant 200$ nm) for 500 h, with samples being removed at 50 h intervals. Further samples of **F0–F5** were fully immersed in sealed containers of 2 M HCl, 2 M NaOH and distilled water for 28 d. Separate containers were used for each sample of **F0–F5** in each medium to avoid cross-contamination.

2.5. Characterisation studies

All samples were individually stored in the absence of light at ambient temperature. No evidence was observed for loss of sample integrity by visible or infrared spectroscopy during storage.

2.5.1. Infrared spectroscopy

All initial and degraded films were examined using diffuse reflectance infrared spectroscopy in the 4000–400 cm^{-1} range on a Nicolet Avatar 360 FTIR**.** Attempts to produce samples of identical surface area suggested significant errors in such an approach which were compounded by the differing reflectance intensity resulting from small changes in surface quality. Thus spectra were obtained from samples of comparable surface area mounted against a dry KBr background.

2.5.2. Colorimetry

Assessment of colorimetric properties was made using a GregtagMacbeth SpectroEye spectrophotometer. Data was recorded using the CIELab system with presented data representing an averaged response from ten sample points within the polymer film.

2.5.3. $^{31}P\{^1H\}$ NMR

Samples were prepared by swelling ~100 mg of polymer in 1–2 cm^3 toluene for 1 d, before adding 1 cm^3 of C_7D_8 for internal referencing. Significant peak broadening did not result from the high viscosity of these materials. However, the low phosphorus content required prolonged data accumulation ($\sim 2 \times 10^4$ scans) limiting the number of samples that could realistically be studied. Thus, initial **F1** and **F2** films and the corresponding materials after 500 h UV irradiation were considered. NMR spectra were obtained using a JEOL FT multinuclear instrument tuned to phosphorus at 81.1 MHz. Broad band decoupling corresponding to the proton resonance region was applied to eliminate ^1H coupling. All samples were externally referenced to 85% phosphoric acid.

3. Results and discussion

3.1. Metal complexes

Following the seminal work of Venanzi [11–13] numerous examples of nickel(II) complexes containing tertiary phosphine ligands have been reported [14]. This body of material fully elucidates the potential to form both square planar (diamagnetic) and tetrahedral (paramagnetic) complexes with geometry and colour being dependent on the nature of both phosphine and metal salt present. Progressive increases in air stability have been recognised on transition from tertiary alkyl- to tertiary aryl-phosphine ligands. Complexes of the thiocyanate anion produce red-orange phosphine complexes which are square planar and diamagnetic; the latter property allowing nuclear magnetic resonance characterisation of the complexes as a pure materials and within polymer matrices. Alkyldiphenyl- and alkenyldiphenyl-phosphine complexes of this salt are considered as relatively robust, with negligible hydrolysis or oxidation occurring for the solid complexes on indefinite exposure to air. Thus, the series of complexes of the type $Ni(NCS)_2(PPh_2R)_2$ [R = methyl (**1**), vinyl (**2**), allyl (**3**), but-3-enyl (**4**), pent-4-enyl (**5**)] have been prepared for incorporation with zinc stearate into polystyrene matrices. Published data confirms the structure and purity of the square planar complexes **1–5** [15].

Thermogravimetric analyses indicate that **1–5** show no propensity to undergo decomposition below 200°C under nitrogen, (Fig. 1). Facile mass loss is recorded for

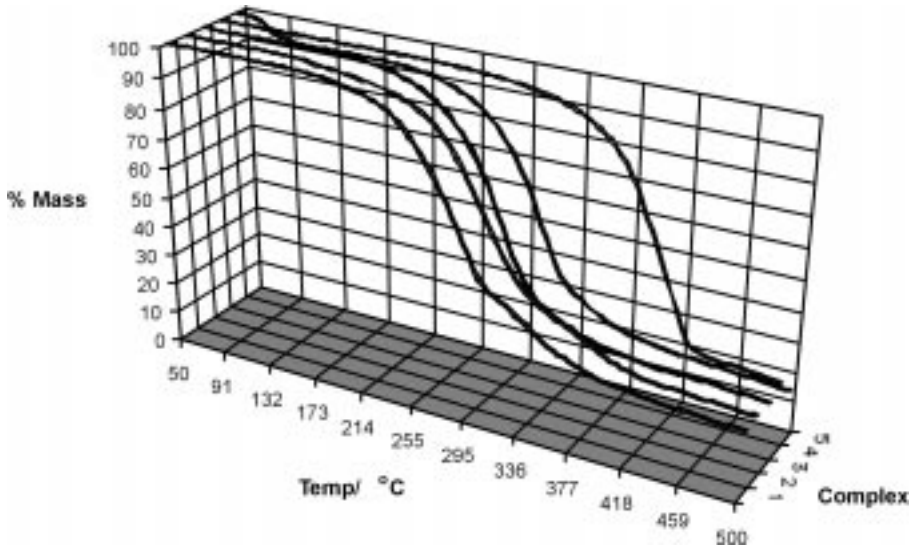

Fig. 1. Thermogravimetric curves for complexes **1**–**5**.

complex **5**; however, this complex was obtained by recrystallisation as solvated **5**.0.5CH_2Cl_2. The observed mass loss of 6.5% corresponds well with the predicted solvent loss (7.0%), whilst the temperature range for this mass decrease of 65–110°C suggests desolvation rather than a high activation energy decomposition process. Therefore, it may be assumed that the preparation of polymer films involving **1**–**5** may reasonably employ elevated temperatures in vacuo or under nitrogen without significant complex decomposition.

UV–VIS spectroscopy shows that the principal absorbance bands in complexes **1**–**5** can be readily assigned to (i) metal-centred d → d transitions of low molar extinction coefficient at 630 nm and (ii) more intense bands resulting from $\pi \rightarrow \pi^*$ transitions derived from the phenyl ligand substituents at 390 nm. Both transitions appear insensitive to modifications in the phosphine substituent R. Fluorescence and phosphorescence studies indicate that neither metal- or π-centred absorbances result in significant fluorescence/phosphorescence either from irradiation at wavelengths corresponding to absorbance maxima or as a consequence of other irradiation in the 300–800 nm region. This absence of significant singlet and triplet states suggests that UV–VIS irradiation of the complexes in solution or within polymer materials will not enhance free radical decomposition processes. Moreover, such complexes offer the potential for the rapid deactivation of singlet and triplet radical species via non-radical routes.

3.2. Polymer films

Polystyrene films **F0**–**F5** incorporating zinc stearate and complexes **1**–**5** and are readily prepared by the addition of complexes and zinc salts to toluene slurries of polystyrene (Table 1). Thermal desolvation in vacuo followed by hot melt pressing generates films of comparable quality and low residual solvent in which both metal compounds are visually well dispersed. Diffuse

Table 1
Physical and spectroscopic properties of films **F0**–**F5**

Polymer film	Additive content	Thermal analysis (% mass loss)	Film thickness (mm (st. dev.))	Infrared[a]		
				ν(NCS) (cm^{-1})	ν(C=O)	ν(C↔C)
F0	2% $Zn(stearate)_2$	0.27	0.251 (0.034)	–	1545	1943, 1867, 1803
F1	2% $Zn(stearate)_2$ + 3% **1**	0.53	0.256 (0.028)	2093	1541	1957, 1872, 1799
F2	2% $Zn(stearate)_2$ + 3% **2**	0.44	0.241 (0.033)	2080, 2153w	1541	1942, 1870, 1801
F3	2% $Zn(stearate)_2$ + 3% **3**	0.30	0.260 (0.059)	2083, 2152w	1541	1943, 1871, 1804
F4	2% $Zn(stearate)_2$ + 3% **4**	0.41	0.278 (0.024)	2079	1543	1943, 1869, 1802
F5	2% $Zn(stearate)_2$ + 3% **5**	0.40	0.273 (0.028)	2083 2156w	1542	1953, 1872, 1806

[a] Bands of strong intensity unless indicated.

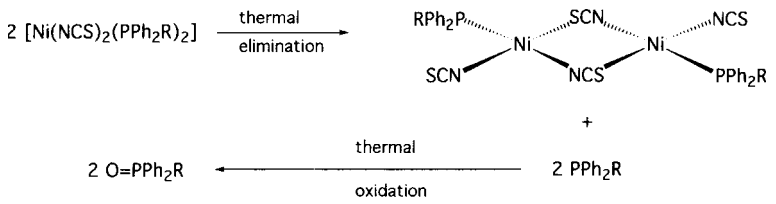

Scheme 2. Proposed thermal elimination process occurring during the formation of **F2**, **F3**.

reflectance FT infrared spectroscopy effectively characterises all components of the films by the facile recognition of ν(NCS) and ν(CO) bands of nickel and zinc compounds as well as the extensive absorbances associated with polystyrene. The ν(NCS) absorbances of **F1**–**F5** (2079–2093 cm^{-1}) are shifted slightly from those of **1**–**5**. To confirm the integrity of **1**–**5** within **F1**–**F5**, it is important that such shifts are rationalised. Thiocyanate anions are known to form weak Lewis base/Lewis acid interactions with aromatic species, and such a sulfur-centred interaction with the polystyrene matrix would justify the observed ν(NCS) shifts from **1**–**5** to **F1**–**F5**. The establishment of thermally induced square planar-tetrahedral equilibria during compression moulding may be excluded by the observation of a single infrared band in the region associated with monodentate thiocyanate co-ordination. Equally complete conversion to tetrahedral geometries would be readily determined by the very different d $\rightarrow$ d transitions that arise from this geometry; the latter normally affording complexes with a green or purple colouration [14]. Within films **F2** and **F3** weak infrared bands are also observed at 2153 and 2152 cm^{-1}, respectively. Thiocyanate absorbances observed at wavenumbers greater than 2100 cm^{-1} are commonly associated with metal bridging NCS^- ions [16–18]. Although such absorbances commonly display an upper limit of 2140 cm^{-1} in discrete complexes, it is reasonable to suggest that this range may be extended to include the observed absorbances of **F2** and **F3** in these significantly different polystyrene matrices. Presumably these bridging species are generated by the thermal displacement of phosphine ligands during thermal desolvation or hot melt pressing (Scheme 2).

3.3. UV photodegradation

The exposure of **F0**–**F5** to UV radiation ($\lambda \geqslant 200$ nm), over a period of 500 h, results in visibly discernible changes in film colouration. Sampling at 50 h intervals allows some assessment of degradation rate, which may be studied using diffuse reflectance FTIR, CIELab colour space and $^{31}P\{^1H\}$ NMR. Whilst the qualitative application of diffuse reflectance IR is facile, quantitative evaluation of polymers is complex and influenced by numerous parameters such as surface and internal reflectance properties, sample orientation and packing medium [19]. Thus, the infrared spectra obtained for **F0**–**F5** prior to irradiation and during the 500 h exposure to UV radiation cannot be simply overlaid to afford direct comparison. Therefore a process of normalisation at a fixed reference absorbance has been adopted. By this method adequate quantitative analysis may be achieved and it may be assumed that precise sample size, orientation and internal reflectance can be ignored. However, it must be noted that the treatment must be considered most effective for the comparison of bands lying at similar wavelengths, where wavelength dependant background and refraction effects are minimised. Normalisation has thus been applied at the polystyrene-derived phenyl ν(C–C) stretching vibration observed at $\sim$1950 cm^{-1}. This particular absorbance lends itself to the role of internal reference on the basis of its predominant intensity and representation of the bulk polymer matrix. Whilst detailed discussions of the spectral changes which occur during irradiation follow, Figs. 2 and 3 illustrate the infrared spectra obtained as a result of normalisation of raw **F5** infrared data at the $\sim$1950 cm^{-1} ν(C–C) stretching vibration.

Using normalised infrared data it is possible to compare the integrity of the nickel additive and bulk polymer during the irradiation of each film **F1**–**F5**. The ν(NCS) band ($\sim$2080 cm^{-1}) is considered representative of the former and the phenyl stretching ν(C–C) ($\sim$1950 cm^{-1}) of the latter. Thus, the relative stability of the two components may be assessed by the intensity ratio of these two bands (Fig. 4). Linear regression analysis of the ν(NCS)/ν(C–C) ratio for each film, as a function of time, demonstrates a decrease in this ν(NCS)/ν(C–C) ratio and therefore an apparent degradation of the nickel additive. However, the regression analyses determine rates of nickel complex degradation of the order of 10^{-3}% h^{-1}. These calculated rates are similar in magnitude or even within the standard deviation of each calculated rate [20], Fig. 5, indicating that the nickel complexes have good intrinsic photostability and degrade at comparable, if slightly greater, rates than the polymer matrix.

Photodegradation in air invariably involves the incorporation of oxygen containing functionalities including alcohols and a variety of carbonyl species. It has been demonstrated that the comparison of carbonyl and

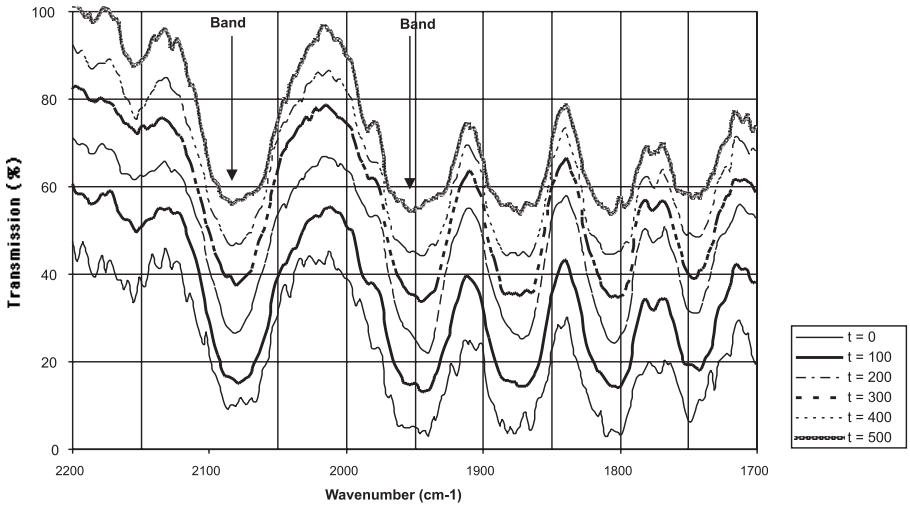

Fig. 2. Normalised infrared spectra of **F5** in the region 2200–1700 cm^{-1}, as a function of irradiation time (spectra offset by 10 cm^{-1}).

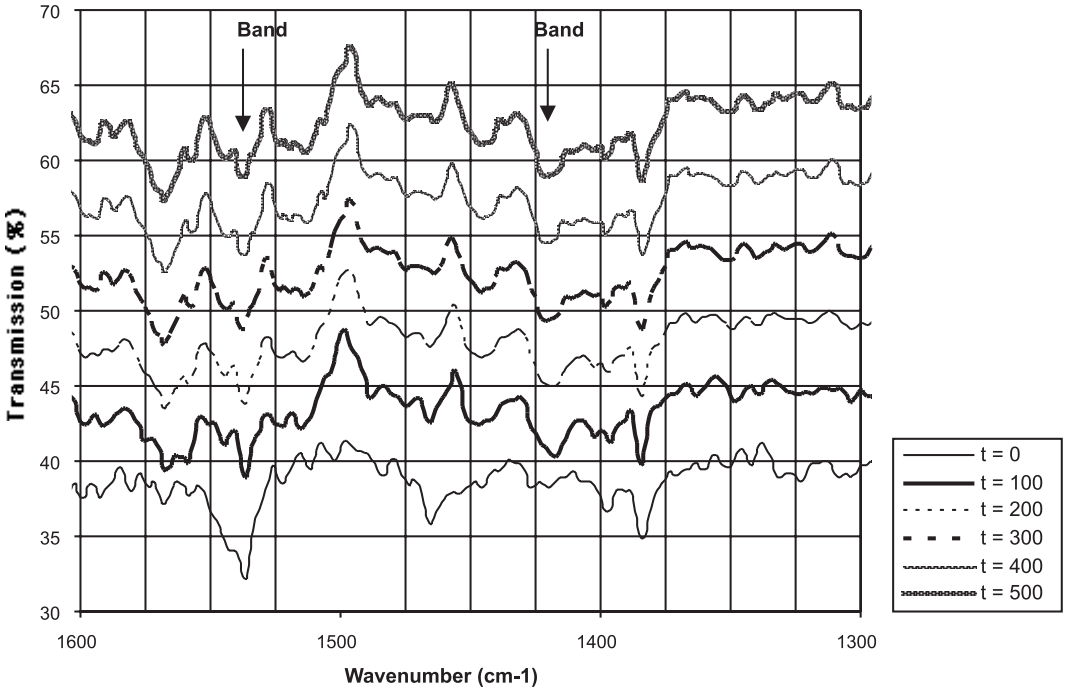

Fig. 3. Normalised infrared spectra of **F5** in the region 1600–1300 cm^{-1}, as a function of irradiation time (spectra offset by 5 cm^{-1}).

hydrocarbon infrared bands is highly effective in quantifying the oxidation of polyolefins [21] and polystyrene systems [22]. In the present study this approach has been hampered by the additional infrared bands derived from nickel and zinc additives, and by the products formed by the degradation of these additives. Thus, as a consequence of UV irradiation loss of the specific stearate ν(CO) at ~1545 cm^{-1} is observed along with the growth of several new absorbances in the 1600–1400 cm^{-1} region, the spectra obtained for **F5** being typical (Fig. 3). A quantitative assessment of the degradation process was attempted by comparison of the stearate-specific absorbance and a new degradation-dependant band at 1420 cm^{-1}. Using this approach, the progression of the

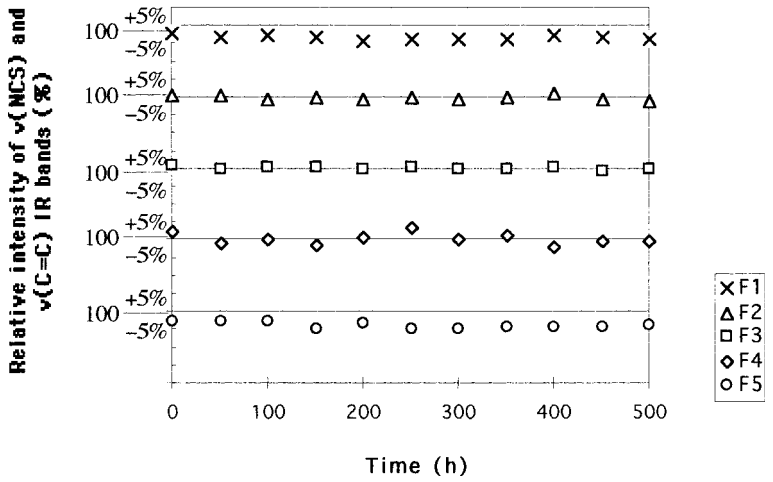

Fig. 4. Infrared reflectance ratio ν(NCS) ($\sim$2080 cm^{-1}) versus ν(C$\backsim$C) ($\sim$1950 cm^{-1}) as a function of irradiation time for **F1**–**F5**.

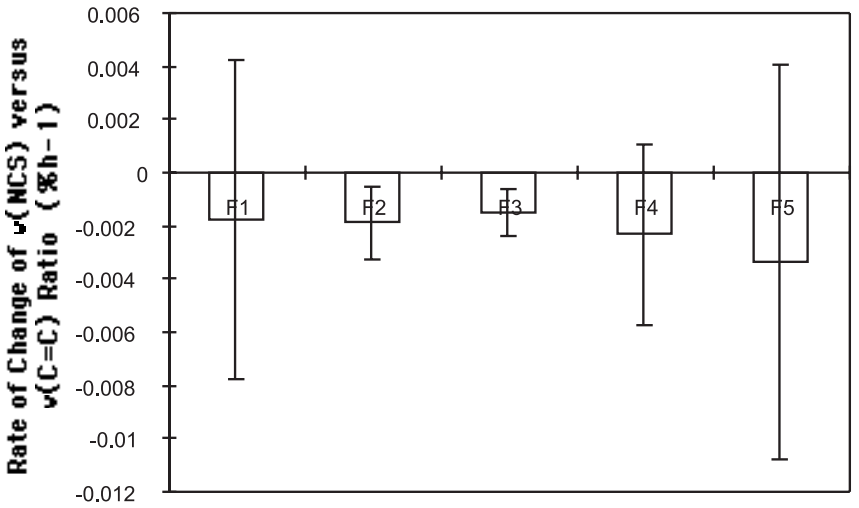

Fig. 5. Linear regression and regression standard deviation for infrared reflectance ratio ν(NCS) versus ν(C$\backsim$C) presented in Fig. 4.

degradation processes is readily apparent (Fig. 6). The tentative application of linear regression analysis produces statistically significant rates, with those of **F2**, **F4** and **F5** being a factor of two greater than that of the nickel-free reference **F0**. In contrast, **F1** and **F3** afford rates that are a factor of two less than **F0** (Fig. 7).

Determination of CIELab colour space for **F0**–**F5** as function of irradiation time indicates that all films display colour changes during irradiation (Fig. 8). These changes may be rationalised by considering the balance of two process; the formation of conjugated organic compounds associated with 'yellowing', and the fading which results from the degradation of **1**–**5**. The latter is likely to cause the conversion of orange-red square planar complexes to less intense tetrahedral or octahedral species that are commonly blue, green or purple. Thus, the nickel-free film **F0** displays only yellowing. **F1** and **F3** fade with small changes in coloration. **F2** appears to lighten and shift to blue/green hues, indicating complex decomposition as the principal chromophore, whilst **F4** and **F5** appear to balance fading and yellowing to produce little overall change. Mechanistic interpretation of these phenomena is complex. However, it appears that the CIELab assessment of **F1** and **F3**, as the film producing least yellowing, concurs that the results of infrared spectroscopy.

$^{31}P\{^{1}H\}$ NMR is recognised as highly diagnostic of both the bonding and chemical environment of phosphorus nuclei. Unfortunately, CP-MAS NMR spectroscopy on these low phosphorus-content solid

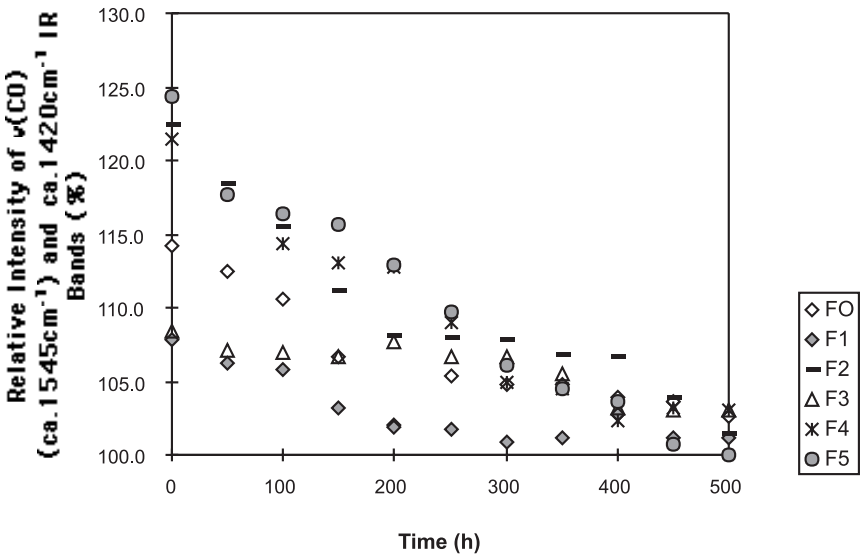

Fig. 6. Infrared reflectance ratio ν(CO) ($\sim$1545 cm^{-1}) versus reflectance observed at $\sim$1420 cm^{-1} as a function of irradiation time for **F0**–**F5**.

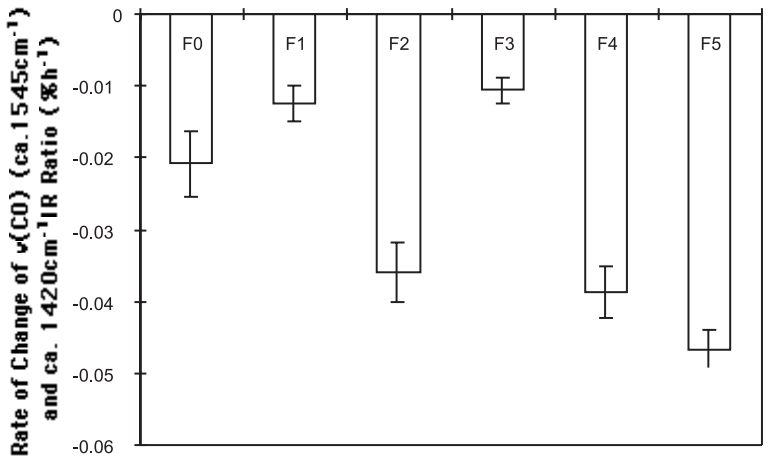

Fig. 7. Linear regression and regression standard deviation for infrared reflectance ratio ν(CO) ($\sim$1545 cm^{-1}) versus reflectance observed at $\sim$1420 cm^{-1} presented in Fig. 6.

polymers would be impractical, forcing the preparation of viscous C_7D_8 swollen samples. Even using this technique, the low signal response of the ^{31}P nucleus, its long NMR relaxation time and the low phosphorus concentration within the films **F1**–**F5**, all result in the need for extended FT accumulation to achieve meaningful data. As a consequence, data was obtained from four samples, consisting of films **F1** and **F2** prior to irradiation and after a full 500 h exposure to UV radiation. To aid spectral interpretation additional data was obtained from the precursor complexes, **1** and **2**, and several potential phosphine oxide degradation products (Fig. 9). Idealised experimental conditions would require phosphorus NMR spectroscopy to be observed for these three groups of materials (polymers, metal complexes and phosphine oxides) under the same experimental conditions. However, in view of the extended accumulations required for **F1** and **F2**, practically demands that similar conditions are not mimicked by the required reference spectra. Thus, $^{31}P\{^1H\}$ NMR data for phosphine oxides was obtained from moderately concentrated solutions (10^{-2}–10^{-3} M) of C_7D_8. **1** and **2**, which are poorly soluble in toluene, could be studied at similar concentrations in $CDCl_3$.

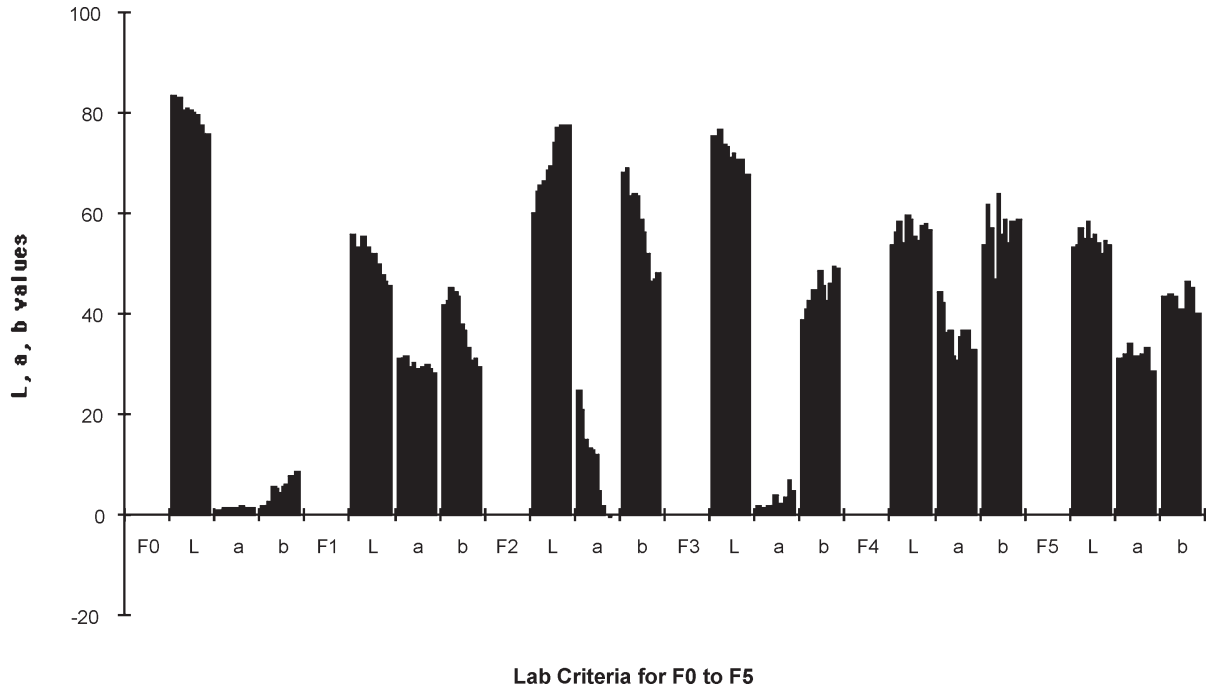

Fig. 8. CIELab data obtained for **F0**–**F5** as a function of irradiation time.

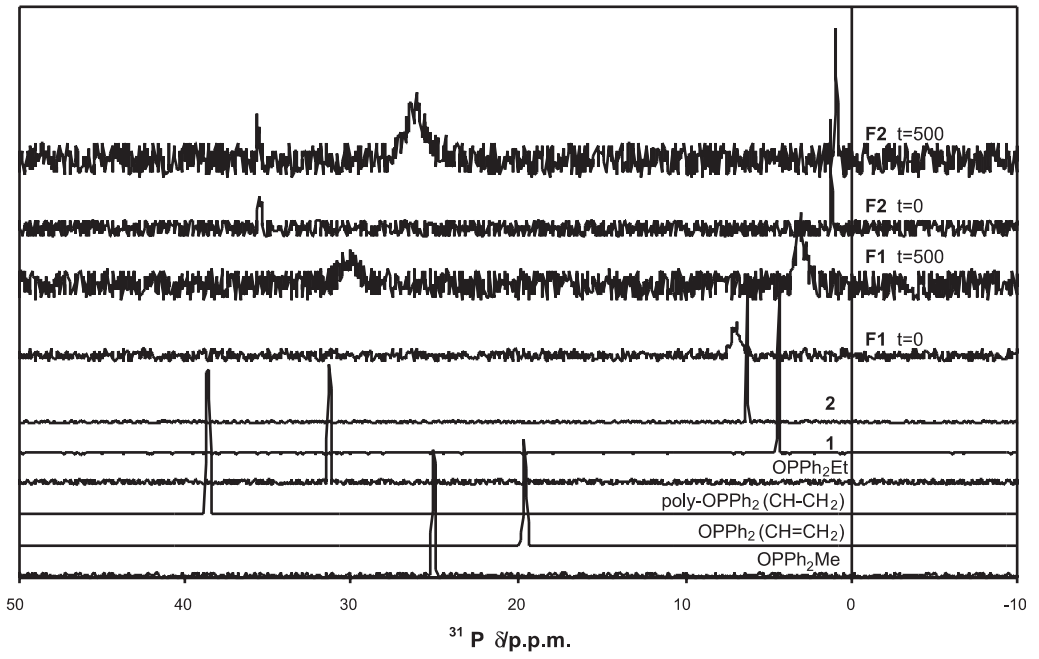

Fig. 9. $^{31}P\{^{1}H\}$ NMR spectra for **F1** and **F2** at $t = 0$ and 500 h, with reference spectra for complexes **1** and **2**, and phosphine oxides.

The observed reference $^{31}P\{^{1}H\}$ NMR resonances, Table 2, fall broadly into two groups. Resonances in the ~0–10 ppm region may be assigned the nickel complexed phosphine ligands [15], whilst those from ~20–40 ppm correspond to phosphine oxides ([23] and references therein). It is immediately evident that the **F1** and

Table 2
$^{31}P\{^{1}H\}$ NMR data for **F1** and **F2** at $t = 0$ and 500 h, with reference spectra for complexes **1** and **2**, and phosphine oxides

Material	Observed $^{31}P\{^{1}H\}$ resonances[a], δ_P	
	$[Ni(NCS)_2(PPh_2R)_2]$	$OPPh_2R$
F1 $t = 0$	6.9	
F1 $t = 500$	3.0	~29 br
F2 $t = 0$	1.2	35.5
F2 $t = 500$	0.9	~25 br, 35.6
Complex **1**[b]	4.4	
Complex **2**[b]	6.2	
$OPPh_2Me$		25.1
$OPPh_2(CH{=}CH_2)$		19.6
Poly-$OPPh_2(CH–CH_2)$		38.6
$OPPh_2Et$		31.3

br: broad.
[a] C_7H_8/C_7D_8 with ext. 85% H_3PO_4 reference.
[b] From Ref. [15], $CDCl_3$ with ext. 85% H_3PO_4 reference.

F2 polymer samples do not relate precisely to their respective reference data, although the resonances, shifted by a few ppm, can be assigned to complexed phosphines and phosphine oxides. Before moving to detailed interpretation of these spectra it is worth discussing the origins of these discrepancies and justifying the integrity of the data presented. NMR spectroscopic data is in general terms highly comparable. However, the recourse, by necessity, to different solvent media introduces secondary effects that are compounded by the use of external referencing. Thus, shifts will occur between nickel phosphine complexes **1** and **2** and their polymer analogues **F1** and **F2**. These are consequences of electric field effects in the $CDCl_3$ solvent of the former, and magnetic anisotropy in the polystrene/C_7D_8 medium of the latter [24]. Whilst these effects are less significant in comparisons between the respective media of **F1** and **F2**, and the phosphine oxides species, it has been demonstrated that the latter are particularly susceptible to chemical shifts resulting from hydrogen bonding [25]. Thus, the inevitable accumulation of oxidised species during photodegradation will clearly result in some shift between the phosphine oxide standards and observed polymer data. Moreover, the formation of even trace quantities of paramagnetic nickel(II) during film formation or degradation has the potential to modify the field positions of the observed resonances by contact or induced shifts.

Consideration of $^{31}P\{^{1}H\}$ NMR spectra from **F1**, **F2**, **1** and **2** suggest that nickel complexed phosphines, **1** and **2**, comprise the principal phosphorus-containing components of **F1** and **F2**, respectively. The additional $^{31}P\{^{1}H\}$ NMR resonance observed for film **F2** at $\delta_P =$ 35.5 ppm is in accord with the formation of phosphine oxide. The shift does not concur with the presence of diamagnetically deshielded vinylic species, and it is therefore realistic to propose that free phosphine liberated in the formation of **F2**, Scheme 2, undergoes oxidation and thermally initiated polymerisation during compression moulding to afford poly-$OPPh_2(CH–CH_2)$. Degraded **F1** and **F2** continue to show strong resonances corresponding nickel complexes **1** and **2** with additional very broad resonances at ~29 and 25 ppm, respectively.

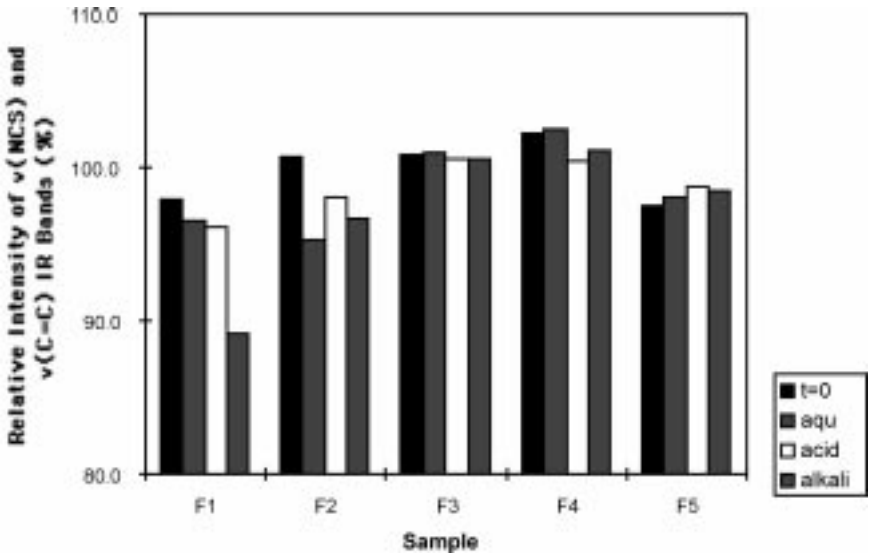

Fig. 10. Infrared reflectance ratio ν(NCS) (~2080 cm^{-1}) versus ν(C⟛C) (~1950 cm^{-1}) for **F1**–**F5** on exposure to aqueous, acidic and alkaline media.

Again these resonances to not correspond directly with those obtained for reference phosphine oxides, but lie within the region associated with such species. Numerous studies have demonstrated the propensity of transition metal co-ordinated phosphines to undergo oxidation to the either free phosphine oxide or its complexes [8–10]. Reactions rates may not be significant at ambient temperature, but at elevated temperatures or in the presence of peroxides oxidation can be rapid. Indeed the laboratory preparation of phosphine oxides is readily achieved by peroxide oxidation [26]. The latter reactivity may provide the key to the photostabilisation properties of **1**–**5**; the facile and stoichiometric consumption of peroxides formed during photodegradation is amongst the most effective forms of stabilisation. Since phosphine oxides are highly stable and unlikely to undergo further decomposition their participation in subsequent free radical initiation will be minimal.

3.4. Solution stability

Polystyrenes are particularly unstable to solvent attack, but also show significant permeability to water, mineral acids and alkalis [6]. Thus, the stability of the polymer and additives contained within **F0**–**F5** has been evaluated prior to, and after 28 d exposure to water, dilute (2M) HCl and dilute (2M) NaOH. Comparable

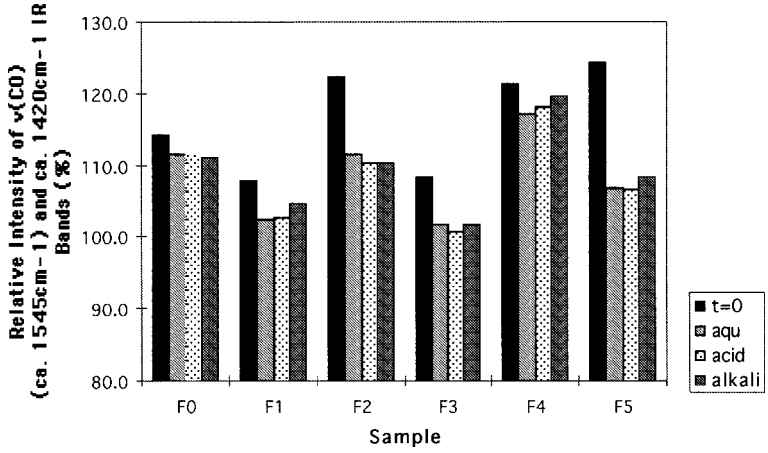

Fig. 11. Infrared reflectance ratio ν(CO) ($\sim$1545 cm^{-1}) versus reflectance observed at $\sim$1420 cm^{-1} for **F0**–**F5** on exposure to aqueous, acidic and alkaline media.

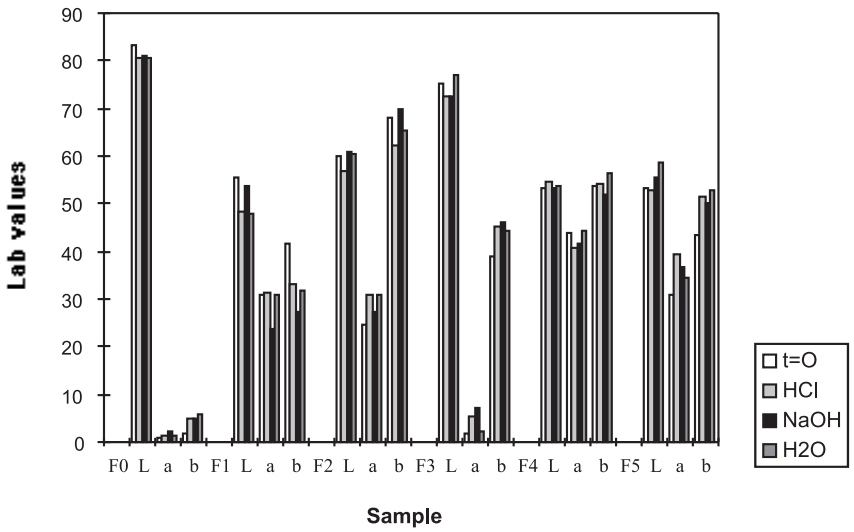

Fig. 12. CIELab data obtained for **F0**–**F5** on exposure to aqueous, acidic and alkaline media.

infrared spectroscopic and CIELab colour space measurements have been made to those employed in the preceding photodegradation studies. It is apparent that leaching of both nickel and zinc additives occurs during the test period (Figs. 10 and 11). These processes are significant and similar in all films. Moreover, few differences are observed between the effects of H_2O, HCl and NaOH. It may therefore be concluded that [H_2O] rather than [H^+] or [^-OH] is rate determining, with the leaching of intact additives and [M^{2+}] ions being the principal processes. Colour leaching of the orange-red chromophores of **1**–**5** is also apparent from CIELab colour space measurements (Fig. 12). Changes in *L*, *a* and *b* parameters are small over this prolonged exposure. It is not possible to firmly establish the chromophores that replace degraded **1**–**5**, since the tetrahedral and octahedral species likely to result from hydrolysis display extinction coefficients for their visible spectral bands which are approximately one order of magnitude lower that those of square planar **1**–**5**.

4. Conclusions

Nickel(II) phosphine complexes may be used as photostabilising additives in polystyrene. Diffuse reflectance IR spectroscopy and CIELab measurements provide effective evaluation of photostability. Behaviour varies with the phosphine substituents present, those containing methyldiphenyl- and allyldiphenyl-phosphines show enhanced stability, other alkenyldiphenylphosphine complexes are photoinitiators. $^{31}P\{^1H\}$ NMR suggests the principal mode of reactivity is phosphine oxidation by peroxides. All polymer films show reasonable tolerance to prolonged exposure to aqueous, acid and alkaline environments.

Acknowledgements

Mr. P. Warren, Drs. P. Schofield and J. Robinson are thanked for their efforts in obtaining NMR, thermogravimetric and phosphorescence/fluorescence data, respectively.

References

[1] Minagawa M. Polym Degrad Stab 1989;25:121.
[2] Allan JR, Carson BR, Wood IJ. Eur Polym J 1996;32:511.
[3] Andrei C, Andrei G, Moraru M, Moise G. Polym Degrad Stab 1999;64:165.
[4] Davis J. In: Pritchard G, editor. Plastic additives: an A–Z reference. London: Chapman and Hall, 1998. p. 277–86.
[5] Scott G. Mater Plast Elast 1973;39:774.
[6] Svec P, Rosík L, Horák Z, Vecerka F. Styrene-based plastics and their modification. Chichester: Ellis Horwood; 1990.
[7] Al-Malaika S, Scott G. Eur Polym J 1983;19:241.
[8] Godfrey SM, Kelly DG, McAuliffe CA, Pritchard RG. J Chem Soc Dalton Trans 1993:2053.
[9] Yoke JD, Schmidt DD. J Am Chem Soc 1971;93:637.
[10] Sznajder J, Jablonski A, Wojciechowski W. J Inorg Nucl Chem 1979;41:305.
[11] Venanzi LM. J Chem Soc 1958:719.
[12] Venanzi LM. J Chem Soc 1961:2705.
[13] Venanzi LM. J Chem Soc 1962:693.
[14] Sacconi L, Mani F, Bencini A. In: Wilkinson G, Gillard RD, McCleverty JA, editors. Comprehensive co-ordination chemistry. Oxford: Pergamon, 1987 [Chapter 50].
[15] Coles SJ, Faulds P, Hursthouse MB, Kelly DG, Ranger GC, Walker NM. J Chem Res 1999;418S:1811M.
[16] Burmeister JL. Coord Chem Rev 1971;6:205.
[17] Norbury AH. Adv Inorg Radiochem 1975;17:248.
[18] Bailey RA, Kozak SL, Michelson TW, Mills WN. Coord Chem Rev 1971;6:407.
[19] Garton A. Infra-red spectroscopy of polymer blends, composites and surfaces. Munich: Hanser; 1992.
[20] Miller JC, Miller JN. Statistics for analytical chemistry, 3rd ed. Chichester: Ellis Horwood, 1993. p. 110–2.
[21] Rabek JF. Experimental methods in polymer chemistry. Chichester: Wiley; 1990.
[22] Allen NS. Degradation and stabilisation of polyolefins. London: Applied Science; 1983.
[23] Maier L. In: Maier L, Kosolapoff GM, editors. Organic phosphorus compounds, vol. 1. New York: Wiley-Interscience, 1972 [Chapter 1].
[24] Harris RK. Nuclear magnetic resonance spectroscopy. Harlow: Longman; 1987.
[25] Godfrey SM, Kelly DG, McAuliffe CA. J Chem Soc Dalton Trans 1992:1305.
[26] Shriner RL, Wolf CN. Org Syn 1950;97.
[27] Paisley DM, Marvel CS. J Polym Sci 1962;56:533.
[28] Wu C, Welch FJ. J Org Chem 1965;30:1229.